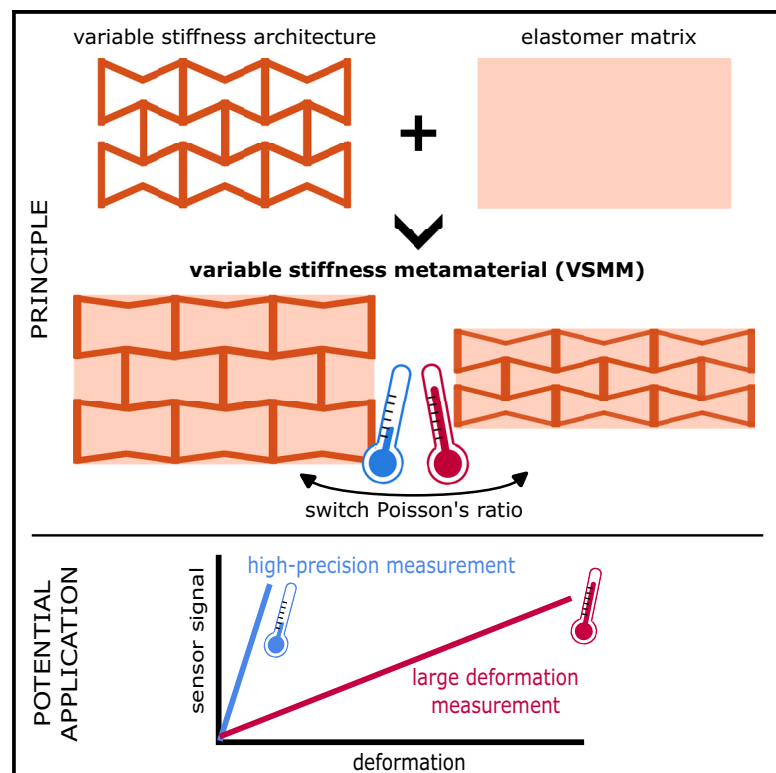**Article**

Variable-stiffness metamaterials with switchable Poisson's ratio

Graphical abstract

Authors

Elze Porte, Nidhi Pashine,
Sree Kalyan Patiballa, Sophia Eristoff,
Trevor Buckner,
Rebecca Kramer-Bottiglio

Correspondence

e.porte@ucl.ac.uk (E.P.),
rebecca.kramer@yale.edu (R.K.-B.)

In brief

This work introduces variable-stiffness metamaterials (VSMMSs) with controllable properties. By stiffening and softening the metamaterial component of VSMMs, the property of the metamaterial structure can be intensified or relaxed. For example, a VSMM with a tunable Poisson's ratio is embedded in a soft sensor to control the sensitivity and strain range of the sensor. VSMMs will expand the capabilities of soft devices through dynamic property modulation.

Highlights

- Variable-stiffness metamaterials (VSMMs) are tunable-response composites

- VSMMs enable on-demand control and intensification of metamaterial properties

- A VSMM with a tunable Poisson's ratio is demonstrated

- A VSMM is embedded in a soft sensor to tune the strain range and sensitivity

Explore
2
Early prototypes with exciting performance and new methodology

CellPress

Article

Variable-stiffness metamaterials with switchable Poisson's ratio

Elze Porte,[1,2,5,*] Nidhi Pashine,[2,3] Sree Kalyan Patiballa,[2,4] Sophia Eristoff,[2] Trevor Buckner,[2] and Rebecca Kramer-Bottiglio[2,*]

[1]Department of Mechanical Engineering, University College London, London WC1E 6BT, UK
[2]Department of Mechanical Engineering and Materials Science, Yale University, New Haven, CT 06511, USA
[3]Department of Physics, Syracuse University, Syracuse, NY 13244, USA
[4]Department of Mechanical Engineering, University of Alabama, Tuscaloosa, AL 35487, USA
[5]Lead contact
*Correspondence: e.porte@ucl.ac.uk (E.P.), rebecca.kramer@yale.edu (R.K.-B.)
https://doi.org/10.1016/j.device.2024.100570

THE BIGGER PICTURE Metamaterials are engineered to exhibit unusual properties, such as material expansion when contraction is expected. Typically, metamaterials have a single response (e.g., always expand), but tuning the intensity of this response (e.g., sometimes expanding, sometimes contracting) is valuable for adaptability and could enhance the adaptability of soft robots and wearables. We develop a variable-stiffness metamaterial (VSMM) that can switch between its "usual" material properties and those substantially altered by metamaterial action. We achieve the tunable properties by embedding a mechanical metamaterial with variable stiffness properties into a soft elastomer matrix. Using soft, stretchable sensors as an example, we demonstrate how the property switching allows the sensors to adapt to different sensitivity and strain range requirements.

SUMMARY

Mechanical metamaterials are structured materials designed to exhibit unconventional mechanical responses. Most mechanical metamaterials have a single material response, but the ability to tune the intensity of a programmed response is useful to enhance the adaptability of the metamaterials to varying application requirements. This work presents variable-stiffness metamaterials (VSMMs) made from a thermally responsive, variable-stiffness Field's metal-silicone composite embedded in a soft silicone elastomer. We investigate VSMMs with different metamaterial structures and constituent material stiffness ratios, and we demonstrate that the VSMM properties are dominated by the embedded metamaterial in a stiff state and the host elastomer in a soft state. We showcase the utility of the VSMM by producing capacitive sensors that can switch between property states: high measurement sensitivity with limited deformations (<10%) or low sensitivity with large deformations (>60%).

INTRODUCTION

Metamaterials can broadly be described as structured materials with bulk properties that differ from the properties of their constituent materials.[1] Metamaterials have been shown to possess unconventional properties, such as a negative Poisson's ratio,[2–5] negative thermal expansion coefficient,[6,7] and nonreciprocity.[8,9] Mechanical metamaterials are a sub-class of metamaterials that exploit motion, deformations, stresses, and mechanical energy.[1] Mechanical metamaterials have been used to augment the properties of soft material systems for specific applications. For example, a negative Poisson's ratio property has been utilized to improve the sensitivity of soft stretch sensors,[10–12] and kirigami principles have been used to design a snake-inspired

crawling robot[13] and inflatable soft actuators with unusual deformations.[13,14]

While many mechanical metamaterials have a fixed structure and therefore a fixed mechanical response, there is a growing interest in metamaterials that can exhibit more than one mechanical response.[1,15–21] For example, bistable mechanisms have been used to switch between rigid and flexible material states of foldable origami structures[15] (i.e., the structure has load-bearing capabilities when the mechanism is locked and free deformation is possible when unlocked),[15] and variable-stiffness materials have been used to adjust how forces travel through a material structure to achieve different deformation responses in the system.[16] Such approaches sought to tune the directionality of a mechanical response. Herein, we are interested in the
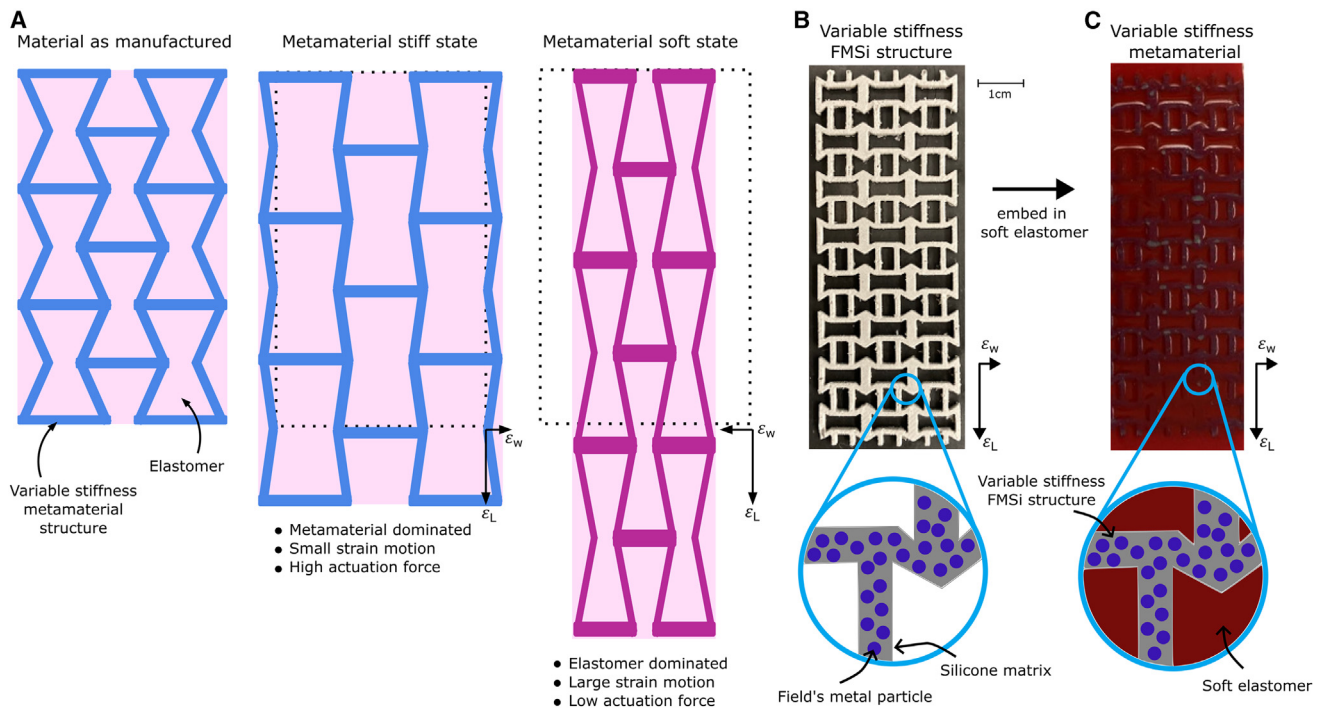
Device
Article

Figure 1. Variable-stiffness metamaterial principles
(A) Overview of the principle of a variable-stiffness metamaterial.
(B) Example of a mechanical metamaterial structure made from FMSi.
(C) Embedded metamaterial to create a variable-stiffness metamaterial.

use of variable-stiffness materials (i.e., variable Young's modulus) in mechanical metamaterials to tune the intensity of a mechanical response.

Rigidity-tuning behavior can be achieved by a variety of means, such as by using stimuli-responsive materials,[22–24] mechanical locking systems,[25,26] antagonistic actuator couplings,[27,28] and jamming effects.[29–32] Phase-changing materials that transition from rigid to soft via a thermal response are a popular approach to stiffness change, as the system design typically has a limited number of components and the effect can be regulated through Joule heating. This strategy has brought about a series of advancements toward the development of phase-changing composites, i.e., materials that have gained some added functionality via the inclusion of an additive with phase-changing properties, such as wax or low-melting-point metallic particle fillers.[33–35] Out of these examples, the most drastic stiffness ranges are provided by fusible metallic alloys, which transition from a rigid metallic solid at room temperature to a dense liquid when heated. Particles of one such alloy, Field's metal (FM), can be added to highly extensible materials, such as silicone rubber.[33] Such a composite benefits from substantial increases in Young's modulus in room temperature environments (stiff state) yet retains access to the flexibility inherent in the matrix material via reversible heating and melting of the internal phase-changing additive (soft state).

In this work, we introduce variable-stiffness metamaterials (VSMMs) (Figure 1A). Mechanical metamaterials are often open structures, where the shape of the voids or cuts determines the material's behavior. Filling the voids with a second material creates a composite material, where the combined material behavior is based on the rule of mixtures, which predicts that the global material properties of a composite will be an average of the constituent material properties proportional to the volume ratio of the constituent materials.[36–38] For a metamaterial, this means that a different stiffness ratio between the metamaterial and the filler material can change its behavior from, for example, auxetic to non-auxetic without changing the metamaterial's structure.[39] Implementing a metamaterial that can change stiffness on demand would mean that the global material properties of the composite can be tuned on demand.

The main benefit of the combined change in stiffness and metamaterial property is for applications where the metamaterial is embedded in continuous bodies, such as capacitive sensors[10–12] and inflatables.[14] In these applications, the stiffness of the metamaterial needs to be much larger than the stiffness of the embedding matrix to exploit the metamaterial properties.[39] The increased stiffness can limit the range of motion and require larger actuating forces. A VSMM can solve these problems by switching between a stiff state when metamaterial action is needed and a soft state when large-range motion and high flexibility are needed (see Figure 1A).

Our VSMM uses a FM-silicone (FMSi) composite to achieve variable stiffness in the metamaterial structure, which is embedded into an elastomer matrix to achieve variable Poisson's ratios with varying temperature. This variable-stiffness mechanism achieves a variation in the Young's modulus of
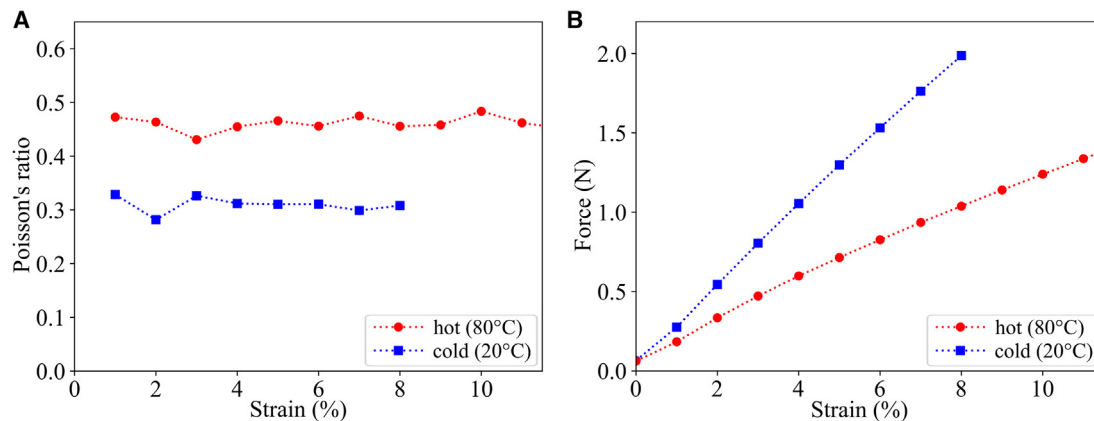
Figure 2. Proof of principle of a thermal responsive variable-stiffness metamaterial
(A) Poisson's ratio and (B) force required to stretch the material ($n = 9$, representative examples shown).

FMSi that is about 5 times as high in its stiff state (room temperature) as in its soft state (>62°C).[33] This VSMM is an example material to introduce the broader concept of VSMMs, which can use different stiffness-changing mechanisms to achieve on-demand control and tunability of metamaterial properties. We investigate the effect of the stiffness change on the Poisson's ratio of the embedded metamaterials for different mechanical metamaterials and a range of stiffness ratios, finding that the VSMM can switch between a stiff, metamaterial-dominated material behavior and a soft, elastomer-dominated material behavior. We demonstrate the utility of the VSMM by making a capacitive sensor that can switch between high sensor sensitivity with a low maximum strain limit and high deformation measurements with lower sensor sensitivity.

RESULTS AND DISCUSSION

VSMM principle

We fabricated a VSMM by embedding a FMSi metamaterial structure inside a soft elastomer matrix. The silicone in the FMSi and the embedded elastomer matrix are both silicone, but for clarity purposes, we refer to the silicone in the FMSi as silicone and the silicone in the soft elastomer matrix as elastomer. FMSi undergoes a drastic stiffness change above the melting temperature of FM, around 62°C.[33] Details of the material manufacturing are described in the experimental procedures.

Figure 1B shows an example of an FMSi metamaterial structure and the final VSMM after embedding the structure in a soft elastomer matrix (Figure 1C). Embedding the metamaterial into the elastomer matrix is an essential step to achieve a variable Poisson's ratio. The hyperelastic Poisson's ratio, which indicates the level of deformation perpendicular to the direction of stretch, can be calculated by[40]

$$\nu_w = -\ln(1+\varepsilon_w)/\ln(1+\varepsilon_L), \quad \text{(Equation 1)}$$

where ν_w is the Poisson's ratio in width direction and ε_w and ε_L are the strains in the width and length directions, respectively.

The Poisson's ratio of the metamaterial in the elastic deformation regime is controlled by the metamaterial structure rather than the constituent material properties. Through embedding the metamaterial, its properties become dependent on both the structure and the composite mechanics of the entire matrix.[39]

Figure 2 shows the proof of principle of the VSMM. Embedding the FMSi metamaterial into a soft elastomer matrix successfully alters the material's behavior at different temperatures. The material shows a Poisson's ratio of 0.5 when heated to 80°C, whereas a reduced Poisson's ratio between 0.3 and 0.4 is measured at room temperature (about 20°C) (Figure 2A). The force required to stretch the warm, softened material to a specific strain is about half of the force required to stretch the material in the cold, stiffened state (Figure 2B). The stiffness change of the VSMM (∼2×) is lower than FMSi materials (∼5×[33]) because the FMSi structure is embedded in an elastomer that does not undergo a stiffness change. Larger stiffness changes in FMSi can be achieved by increasing the metal content,[41] but this reduces the maximum strain at failure. The stiffness change of VSMM can be expected to increase if the ratio FMSi:elastomer of the VSMM can be increased toward FMSi content. The material is prone to breaking at strains above 10% in the stiff state, so measurements are only taken up to approximately 8% strain. In the softened state, the material is able to endure much larger strains (>50%).

Effect of metamaterial structure choice

To further investigate the mechanics of the VSMMs, we tested different structures for the metamaterial and used different constituent materials in the VSMM composite. Four different known metamaterial structures are investigated (Figure 3): a "honeycomb" structure with a Poisson's ratio >1, a "bowtie" (reentrant honeycomb) structure with a negative Poisson's ratio, a kirigami structure with a negative Poisson's ratio, and a "squares" structure with a Poisson's ratio of approximately 0.[5] The measured Poisson's ratios of these four structures are captured in Figure 3B. These four structures are chosen to cover a large spectrum of unusual Poisson's ratios ranging from 1.5 to −0.5. Two structures with a Poisson's ratio of −0.5 are included to investigate different types of mechanisms to achieve negative
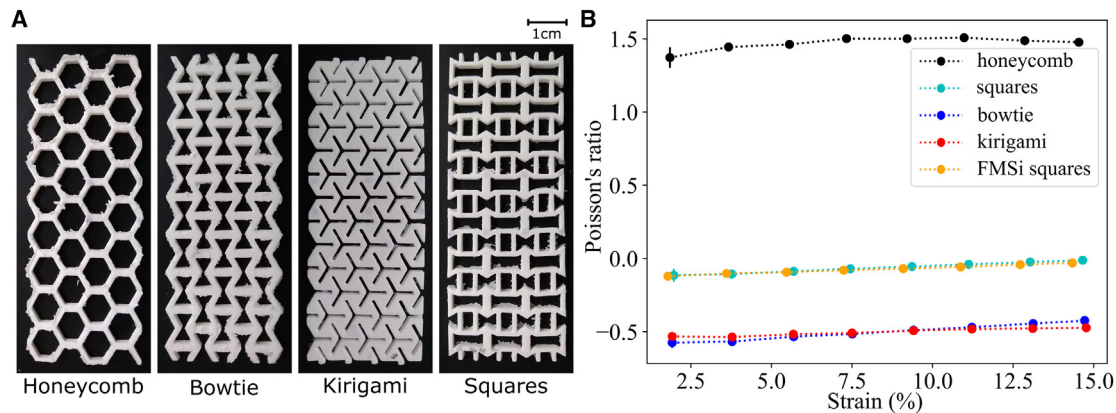
Device
Article

Figure 3. Poisson's ratios of different metamaterial structures
(A) The four different structures.
(B) Poisson's ratios of the four different structures, including tests on an FMSi structure to show independence of material properties ($n = 9$, error bars indicate the standard deviation, and a dashed line was added to guide the reader).

Poisson's ratios. The Poisson's ratio of the squares is measured for structures made from both a soft elastomer (Ecoflex 00-30) and much stiffer FMSi to confirm the Poisson's ratio is independent of constituent material properties. All other structures are only made from soft elastomer.

Figures 4A and 4B show the measured Poisson's ratios of the four metamaterial structures as VSMMs at both the stiff (20°C) and softened (80°C) states. All structures behave as neat silicone in the softened state with a Poisson's ratio close to 0.5 (Figure 4B). The Poisson's ratio changes in the stiff state for three of the structures, with Poisson's ratios above 0.5 for the honeycomb structure and below 0.5 for the bowtie and squares structures (Figure 4A). The embedded kirigami structure shows a Poisson's ratio of 0.5, even though the structure on its own showed a Poisson's ratio of −0.5. The bowtie and kirigami structures initially showed similar Poisson's ratios but then showed different Poisson's ratios as part of the VSMM. This indicates that the change in Poisson's ratio is highly dependent on the chosen structure.

The difference in Poisson's ratio of the embedded bowtie and kirigami structures shows that the composite's Poisson's ratio cannot be predicted from the metamaterial's original Poisson's ratio alone. The difficulty in predicting the behavior is likely due to the different internal stresses for the different structures. For the kirigami structure, the voids in the material become much bigger during stretch compared to the bowtie structure (Figure S1). The voids in the kirigami structure have an increase of about 40% more area than the bowtie structure at the same level of strain (15%). When the metamaterials are embedded in the elastomer, the elastomer will resist the opening of the voids and limit the metamaterial's action.

Effect of constituent materials choice
The effect of the constituent materials is investigated on the bowtie structure since the largest change in Poisson's ratio between the stiff and soft states is achieved with this structure. Based on the rule of mixtures, it is expected that larger stiffness ratios between the metamaterial and matrix material in the cold state result in lower Poisson's ratios since the metamaterial stiff-

ness will dominate the composite behavior. Different stiffness ratios are achieved by changing the constituent elastomers of both the embedding matrix and the FMSi composite. The elastomers are a relatively soft Ecoflex 00-30 (Smooth-On), medium-stiffness Dragon Skin 20 (Smooth-On), and relatively stiff Smooth-Sil 950 (Smooth-On). Three different stiffness ratios between the constituent elastomers are chosen: a low stiffness ratio (1:1) where Dragons Skin 20 is used for both the FMSi structure and embedding matrix, a medium stiffness ratio (1:5, Ecoflex 00-30:Dragon Skin 20, 100% modulus) consisting of a Dragon Skin 20 FMSi composite embedded in Ecoflex 00-30, and a large stiffness ratio (1:27, Ecoflex 00-30:Smooth-Sil 950, 100% modulus) consisting of a Smooth-Sil 950 FMSi composite embedded in Ecoflex 00-30.

Figures 4C and 4D show the Poisson's ratio in both the cold and hot states for the different composite combinations. The graphs indicate that the Poisson's ratio of the embedded material in the cold state is dependent on the stiffness ratio between the metamaterial and the embedding matrix. The lowest Poisson's ratio (about 0.1) is measured for the highest stiffness ratio material, and the highest Poisson's ratio (between 0.4 and 0.5) is measured for the lowest stiffness ratio material, which follows the expected trend based on the rule of mixtures. The high stiffness ratio in the cold state, however, also results in a relatively high stiffness ratio between the metamaterial and the embedding matrix in the softened, hot state. The high stiffness ratio results in a reduced Poisson's ratio around 0.3–0.4 for the high-stiffness material compared to a Poisson's ratio of 0.5 for the low- and medium-stiffness materials. Even though the stiffness of the FMSi metamaterial structure is much lower through the melting of the FM, the stiffness ratio between the stiff Smooth-Sil 950 of the metamaterial and the soft Ecoflex 00-30 of the matrix is sufficiently high to observe the influence of the metamaterial mechanics through a reduced Poisson's ratio.

The relatively large error bars in Figures 4A–4D at low strains may be explained by the ratio of the measurement uncertainty compared to the magnitude of the measured strain. The measurement accuracy of the measurement method is absolute,
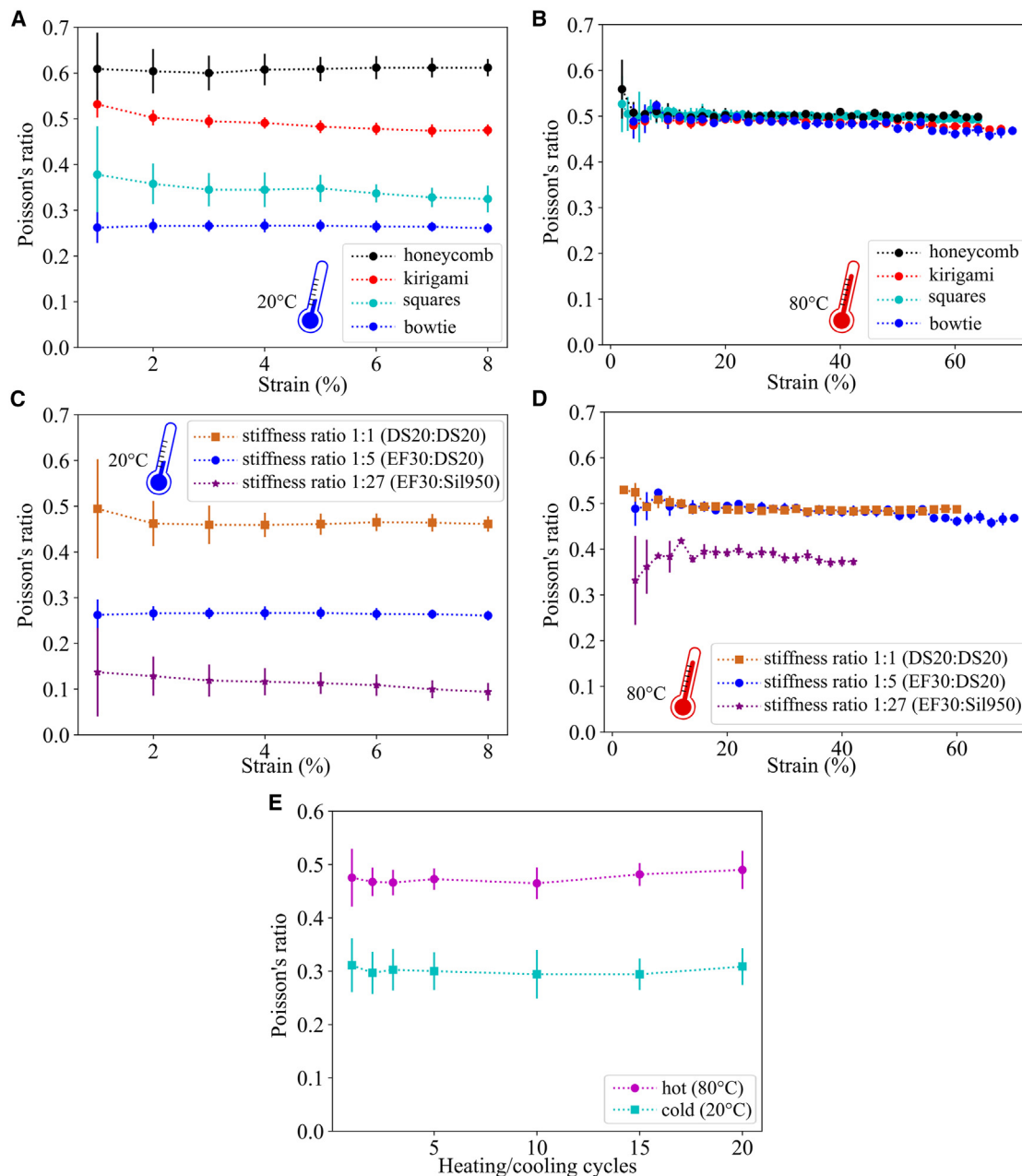
Figure 4. Metamaterial structure choice, constituent material choice and repeatability

(A and B) Poisson's ratios of the four different embedded metamaterial structures in the (A) cold and (B) hot states.

(C and D) Poisson's ratios of the embedded bowtie structure for three different composites using Dragon Skin 20 (DS20), Ecoflex 00-30 (EF30), and Smooth-Sil 950 (Sil950) in the (C) cold and (D) hot states.

(E) Repeatability test results showing the Poisson's ratio for 20 repeated heating and cooling cycles.

For all graphs, *n* = 9, error bars indicate the standard deviation, and a dashed line was added to guide the reader.

which means that for large strains, the relative uncertainty of the measurement becomes smaller.

The VSMM shows repeatable behavior between temperature cycles. The graph in Figure 4E shows that over 20 heating and cooling cycles, the average Poisson's ratios of the squares VSMM remained stable around 0.3 in the cold state and around

0.5 in the hot state. This means that systems with VSMMs can repeatably switch between the different states. Although more elaborate tests over thousands of repeated cycles should be carried out to cover the lifespan of these soft material systems, these initial results where no change is observed in the material's behavior are very promising. In general, the repeatability of a
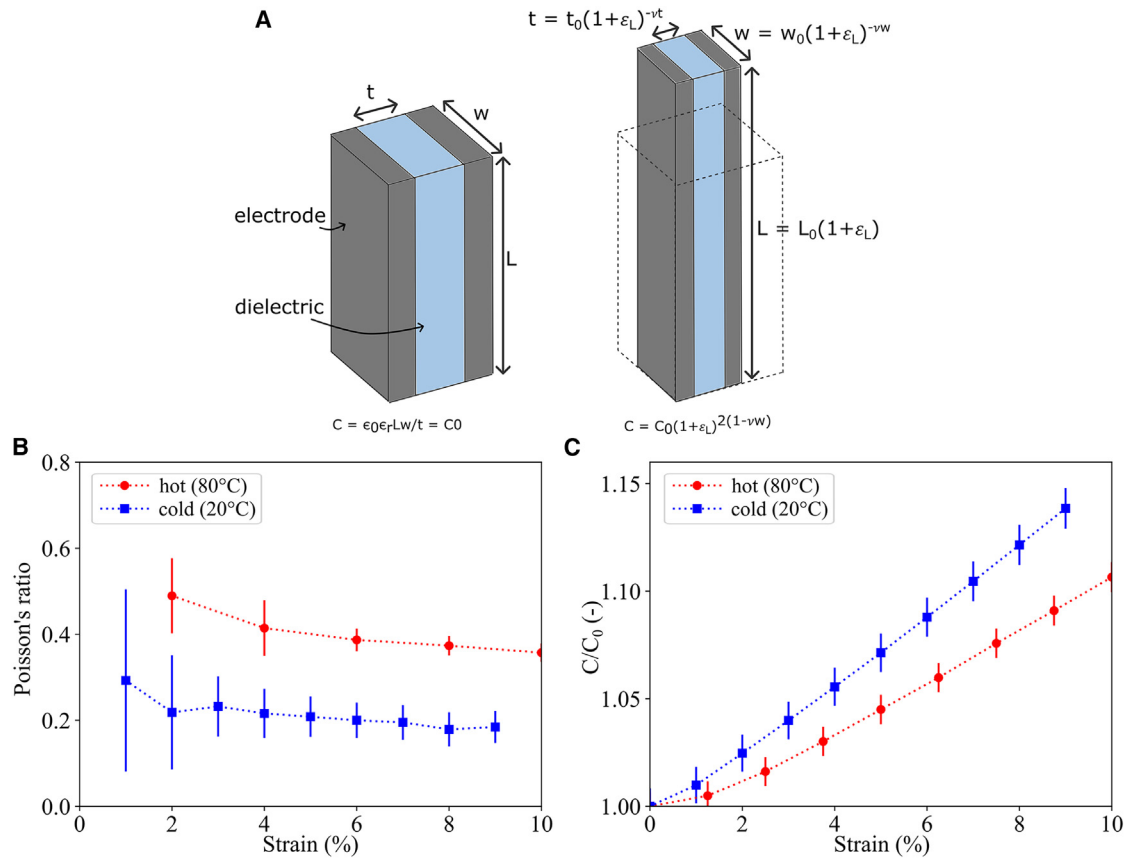
Device
Article

Figure 5. Capacitive sensor case study application
(A) Schematic of a capacitive sensor, including how dimensions relate to measured capacitance.
(B and C) Comparison of sensor data in cold and hot states for (B) Poisson's ratio and (C) normalized capacitance ($n = 9$, error bars indicate the standard deviation, and a dashed line was added to guide the reader).

VSMM is expected to depend on the choice of stiffness-changing mechanism and the bonding properties between the metamaterial and matrix material.

Case study application

A possible application in soft robotics where a VSMM can provide benefits compared to conventional materials is soft capacitive stretch sensors. Capacitive sensors typically have relatively low resolution.[42] Embedding VSMMs in soft stretch sensors can enable switching between a lower-strain state with higher resolution and a higher-strain state with lower resolution. Capacitive sensors consist of two electrodes that are separated by a dielectric layer, as schematically represented in Figure 5A. Soft capacitive sensors are often silicone based, with a neat silicone dielectric layer and conductive particle-filled silicones as electrodes.[42–44] Measurements with capacitive sensors rely on the deformations of the sensors during stretch through[43,44]

$$C = \epsilon_0 \epsilon_r \frac{Lw}{t} \qquad \text{(Equation 2)}$$

with C the measured capacitance, ϵ_0 the permittivity of free space, ϵ_r the relative permittivity, and L, w, and t the length,

width, and thickness of the dielectric layer, respectively. The capacitance measurements directly relate to the effective Poisson's ratio of the dielectric layer since the Poisson's ratio determines the relationship between the stretch in the w and t directions, based on an imposed strain in L and assuming the incompressibility of the dielectric layer[43]:

$$C = C_0(1+\varepsilon_L)^{2(1-\nu_w)} \qquad \text{(Equation 3)}$$

where ε_L is the strain in the L direction and ν_w is the effective Poisson's ratio in the w direction of the dielectric layer. The incompressibility of the dielectric layer means that volume is conserved through $\nu_w + \nu_t = 1$, where ν_t is the Poisson's ratio in the t direction. Reducing ν_w through using VSMMs results in a higher ν_t, which means that as the w reduces less with ε_L, the t reduction increases. Since $C \propto Lw/t$, this combined effect increases the measured capacitance for a given ε_L.

To showcase the potential capabilities of VSMMs, we created a VSMM stretch sensor with tunable strain range and sensitivity properties. The bowtie VSMM is molded onto a soft capacitive stretch sensor to reduce the Poisson's ratio of the sensor on demand. Figures 5B and 5C show the Poisson's ratios and

capacitance measurements of the sensors in cold and hot states. As expected, the Poisson's ratio of the sensors is lower in the cold (~0.2) than in the hot (~0.35) state. The Poisson's ratio of the sensors does not revert to 0.5 in the hot state for two reasons. First, we use the stiffer metamaterial (Smooth-Sil 950 based), which has a Poisson's ratio of 0.4 in the hot state (Figure 4D). Second, the sensors themselves have a Poisson's ratio below 0.5 (~0.3–0.4) because of the addition of graphite to the electrodes.[43]

The difference between the Poisson's ratios in the softened (80°C) and stiffened (20°C) states is sufficiently large to alter the sensitivity of the capacitance measurements. The capacitance change with strain in the cold state is about 50% higher than in the hot state. This measurement sensitivity change is lower than the gauge factor increase achieved in other capacitive sensor metamaterial technologies (90% increase),[42] but optimization of the current system could improve the performance. The sensor in the cold state could not be tested beyond 9% strain because of the high stiffness and potential failure of the FMSi structure. Measurements beyond 60% strain were possible in the hot state. This means that the VSMM successfully achieved changing the material properties of capacitive sensors on demand, with potential applications in soft robotics.

Conclusion and outlook

This work introduces the principle of VSMMs. To demonstrate, we developed a VSMM that can be used in soft systems to switch between different property states, dependent on the stiffness of the metamaterial structure. We showed that the VSMM can switch between behavior that is dominated by the soft elastomer matrix to enable large-strain motion and a high-stiffness state with a substantially altered Poisson's ratio due to the metamaterial's impact on the global material properties. Both the original Poisson's ratio and the structure of the metamaterial determine the Poisson's ratio of the VSMM. The Poisson's ratio can also be altered based on the stiffness ratio between the metamaterial and the filler, with a larger stiffness ratio resulting in a larger contribution of the metamaterial structure to the material properties.

We show the functionality of the VSMM for soft capacitive sensors but envision that this programmable material can have a wide range of applications in soft robots and adaptable materials. For example, an actuator could be programmed to follow different paths with different load-bearing capabilities. VSMMs can be created with any rigidity-tuning material, and the use of other variable-stiffness mechanisms, such as jamming, could increase the switching speed and extend the technology to temperature-sensitive applications, for example, in biomedical and surgical devices. Further development of the materials is required to optimize their use for specific applications, and the suitability of VSMMs to alter other metamaterial actions, such as multistability and shape shifting, can be explored. Inverse design may be a useful tool to design these materials with optimized metamaterial structure and stiffness ratios.

EXPERIMENTAL PROCEDURES

FM particle preparation

The process of preparing FM particles is based on a method previously introduced by the authors in Buckner et al.[45] First, a 2 wt % solution of confection-

ery sodium alginate powder (Modernist Pantry) and deionized water is poured into a 1,000 mL beaker. The mixture, which is thixotropic and behaves like a syrupy gel, is then heated to around 70°C by placing the beaker in a heated silicone oil bath (95°C). Small ingots of FM (Roto144F, RotoMetals) with a total weight of 60 g are placed in the heated medium and allowed to melt for approximately 10 min. Then, a homogenizer (Cole-Parmer LabGEN 850) with a 20 mm diameter saw-tooth generator attachment is turned on at 10,000 rpm for 60 s to break apart the melted FM into small liquid droplets with a mean diameter of 50 μm. A mean particle size of 50 μm was identified for an optimal performance of FMSi in terms of strength and variable stiffness.[46] Once the homogenizer is turned off, the medium vitrifies in place, capturing the FM droplets in suspension to cool. The mixture is then diluted with additional water to allow the solidified particles to sink to the bottom of the beaker. The supernatant is decanted off, and the metal particles are rinsed and then dried in a vacuum chamber overnight. The resulting particles are ready to be used as a composite filler.

Metamaterial manufacturing

Metamaterials are prepared by three-dimensional (3D) printing polylactic acid (PLA) molds for each structure. Thereafter, FM particles are mixed into prepared silicones at 50 vol %. Although a higher-stiffness change may be achieved at higher volume ratios,[41] the FMSi become difficult to mold into the intricate metamaterial structure because of increased viscosity before molding and increased brittleness after curing. Ecoflex 00-30 (Smooth-On) and Dragon Skin 20 (Smooth-On) are prepared with a 1:1 ratio A:B and Smooth-Sil 950 (Smooth-On) with a 10:1 ratio A:B. The FMSi mixture is poured into the molds and placed in a vacuum chamber to remove air bubbles. Excess silicone is scraped from the top with a metal blade. Once the material has cured, the metamaterials are carefully released from the molds and incorporated into a soft elastomer matrix. The metamaterials are placed on a flat surface and covered in the prepared elastomer. A film applicator bar (SH0340, TQC Sheen) is used to level the elastomer with the metamaterial structure. The embedded metamaterial is cut to size along the edges of the metamaterial structure using a surgical knife. To allow easier mounting on the testing machine, the cut along the short edge of the metamaterial is made approximately 5 cm from the edge of the structure.

Metamaterial testing

All the metamaterial samples were tested at room temperature where the FM is in the solid state as well as at 80°C, where the FM is completely melted. The strain in both the L and w directions of the samples is determined by image analysis of a 3 × 3 grid of dots painted on each sample (Figure S2; Note S1). Images of the samples were captured with an imaging system (Grasshopper 3, Point Grey Research). The response of the sample was measured under quasi-static uniaxial strain along their longest dimension using a universal materials tester (Instron 3365). The embedded metamaterial structures are approximately 2 × 30 × 80 mm, and the samples are pre-stretched by 8 mm in the cold state and 60 mm in the hot state to get rid of Mullin's effect. To measure the strain response, the samples are strained by 7.5 mm in the cold state and 55 mm in the hot state. This corresponds to 9% and 68% strain of the embedded metamaterial structure in the cold and hot states, respectively. However, the metamaterial samples often slip during the strain tests, and as a result, the actual material strain is usually limited to 8% and 60% in cold and hot states, respectively. All the strain data presented in this work are an average of three samples, with each sample measured three times.

Sensor manufacturing and testing

Soft capacitive sensors were manufactured following protocols previously developed by the group of Porte et al.[43,47] and White et al.[48] In short, sensors were fabricated with Ecoflex 00-30 (Smooth-On) as base material, and expanded intercalated graphite (EIG) was used as a conductive filler for the electrodes. Expandable graphite flakes (Sigma-Aldrich) were expanded at 800°C and subsequently sonicated in cyclohexane for 1 h at 70% (Q500 1/2″ tip, Qsonica). Large particles were sieved from the mixture using a 212 μm mesh sieve. The mixture was boiled down to approximately 3 wt % EIG. The exact percentage of EIG was measured by weighing a spoonful of the mixture before and after solvent evaporation. For the electrodes, the EIG mixture was manually stirred into the Ecoflex 00-30 at a ratio that resulted in 10 wt % EIG in the electrode after evaporation of the solvent. The EIG-silicone

composite was coated on a PET substrate using a film applicator (500 μm, SH0340, TQC Sheen). After curing, the dielectric silicone was coated on top of the electrode layer (1,000 μm). After curing the dielectric layer, the second electrode layer (EIG-silicone composite) was coated on top of the dielectric layer (500 μm). The final thickness is slightly lower than the coated thickness due to the spreading of the silicone before curing. Sensors were cut to the same size as the metamaterials (30 × 80 mm) with a laser cutter (VLS 2.30, Universal Laser System). Copper foil strips were glued to the sensors with conductive glue to interface the sensors with the testing system. Conductive glue was prepared by mixing Silpoxy (Smooth-On) with the EIG mixture in the same ratio as the electrode layers. Embedded metamaterials were produced as described above. The metamaterial structures were made with Smooth-Sil 950 and embedded in Ecoflex 00-30. The sensors were attached to the metamaterial sample with a thin layer of Ecoflex 00-30. The sensors were tested using the same testing protocol as described in the metamaterial testing section. Capacitance measurements from the sensors were taken during these tests with an LCR meter (Keysight E4980A/AL).

RESOURCE AVAILABILITY

Lead contact
Further information and requests for resources and reagents should be directed to and will be fulfilled by the lead contact, Elze Porte (e.porte@ucl.ac.uk).

Materials availability
This study did not generate new unique reagents.

Data and code availability
All data reported in this paper will be shared by the lead contact upon request. This paper does not report original code. Any additional information required to reanalyze the data reported in this paper is available from the lead contact upon request.

AUTHOR CONTRIBUTIONS

Conceptualization, E.P., S.K.P., and R.K.B.; methodology, E.P., S.E., and T.B.; validation, E.P.; formal analysis, E.P. and N.P.; investigation, E.P., N.P., and S.K.P.; writing – original draft, E.P., N.P., S.K.P., S.E., and T.B.; writing – review & editing, E.P., N.P., S.K.P., S.E., and R.K.B.; visualization, E.P. and N.P.; project administration, E.P.; supervision, R.K.B.; funding acquisition, R.K.B.; resources, R.K.B.

DECLARATION OF INTERESTS

The authors declare no competing interests.

SUPPLEMENTAL INFORMATION

Supplemental information can be found online at https://doi.org/10.1016/j.device.2024.100570.

REFERENCES

1. Bertoldi, K., Vitelli, V., Christensen, J., and Van Hecke, M. (2017). Flexible mechanical metamaterials. Nat. Rev. Mater. *2*, 17066. https://doi.org/10.1038/natrevmats.2017.66.

2. Lakes, R.S. (2017). Negative-Poisson's-Ratio Materials: Auxetic Solids. Annu. Rev. Mater. Res. *47*, 63–81. https://doi.org/10.1146/annurev-matsci-070616.

3. Huang, C., and Chen, L. (2016). Negative Poisson's Ratio in Modern Functional Materials (Preprint at Wiley-VCH Verlag), pp. 8079–8096. https://doi.org/10.1002/adma.201601363.

4. Patiballa, S.K., and Krishnan, G. (2022). On the design of three-dimensional mechanical metamaterials using load flow visualization. Mech. Base. Des. Struct. Mach. *50*, 442–467. https://doi.org/10.1080/15397734.2020.1719506.

5. Patiballa, S.K., and Krishnan, G. (2018). Qualitative analysis and conceptual design of planar metamaterials with negative Poisson's ratio. J. Mech. Robot. *10*, 021006. https://doi.org/10.1115/1.4038977.

6. Qu, J., Kadic, M., Naber, A., and Wegener, M. (2017). Micro-Structured Two-Component 3D Metamaterials with Negative Thermal-Expansion Coefficient from Positive Constituents. Sci. Rep. *7*, 40643. https://doi.org/10.1038/srep40643.

7. Wang, Q., Jackson, J.A., Ge, Q., Hopkins, J.B., Spadaccini, C.M., and Fang, N.X. (2016). Lightweight Mechanical Metamaterials with Tunable Negative Thermal Expansion. Phys. Rev. Lett. *117*, 175901. https://doi.org/10.1103/PhysRevLett.117.175901.

8. Wang, X., Li, Z., Wang, S., Sano, K., Sun, Z., Shao, Z., Takeishi, A., Matsubara, S., Okumura, D., Sakai, N., et al. (2023). Mechanical nonreciprocity in a uniform composite material. Science *380*, 192–198. https://doi.org/10.1126/science.adf1206.

9. Coulais, C., Sounas, D., and Alù, A. (2017). Static non-reciprocity in mechanical metamaterials. Nature *542*, 461–464. https://doi.org/10.1038/nature21044.

10. Jiang, Y., Liu, Z., Matsuhisa, N., Qi, D., Leow, W.R., Yang, H., Yu, J., Chen, G., Liu, Y., Wan, C., et al. (2018). Auxetic Mechanical Metamaterials to Enhance Sensitivity of Stretchable Strain Sensors. Adv. Mater. *30*, 1706589. https://doi.org/10.1002/adma.201706589.

11. Wong, J., Gong, A.T., Defnet, P.A., Meabe, L., Beauchamp, B., Sweet, R.M., Sardon, H., Cobb, C.L., and Nelson, A. (2019). 3D Printing Ionogel Auxetic Frameworks for Stretchable Sensors. Adv. Mater. Technol. *4*, 1900452. https://doi.org/10.1002/admt.201900452.

12. Shintake, J., Nagai, T., and Ogishima, K. (2019). Sensitivity Improvement of Highly Stretchable Capacitive Strain Sensors by Hierarchical Auxetic Structures. Front. Robot. AI *6*, 127. https://doi.org/10.3389/frobt.2019.00127.

13. Rafsanjani, A., Zhang, Y., Liu, B., Rubinstein, S.M., and Bertoldi, K. (2018). Kirigami skins make a simple soft actuator crawl. Science Robotics *3*. https://doi.org/10.1126/scirobotics.aar7555.

14. Jin, L., Forte, A.E., Deng, B., Rafsanjani, A., and Bertoldi, K. (2020). Kirigami-Inspired Inflatables with Programmable Shapes. Adv. Mater. *32*, e2001863. https://doi.org/10.1002/adma.202001863.

15. Kamrava, S., Mousanezhad, D., Ebrahimi, H., Ghosh, R., and Vaziri, A. (2017). Origami-based cellular metamaterial with auxetic, bistable, and self-locking properties. Sci. Rep. *7*, 46046. https://doi.org/10.1038/srep46046.

16. Pashine, N., Nasab, A.M., and Kramer-Bottiglio, R. (2023). Reprogrammable allosteric metamaterials from disordered networks. Soft Matter *19*, 1617–1623. https://doi.org/10.1039/d2sm01284g.

17. Yang, H., and Ma, L. (2018). Multi-stable mechanical metamaterials with shape-reconfiguration and zero Poisson's ratio. Mater. Des. *152*, 181–190. https://doi.org/10.1016/j.matdes.2018.04.064.

18. Bossart, A., Dykstra, D.M.J., Van Der Laan, J., and Coulais, C. (2021). Oligomodal metamaterials with multifunctional mechanics. Proc. Natl. Acad. Sci. USA *118*, e2018610118. https://doi.org/10.1073/pnas.2018610118/-/DCSupplemental.y.

19. Jin, L., Khajehtourian, R., Mueller, J., Rafsanjani, A., Tournat, V., Bertoldi, K., and Kochmann, D.M. (2020). Guided transition waves in multistable

Device
Article

mechanical metamaterials. Proc. Natl. Acad. Sci. USA *117*, 2319–2325. https://doi.org/10.6084/m9.figshare.10048724.v2.y.

20. Ye, M., Gao, L., and Li, H. (2020). A design framework for gradually stiffer mechanical metamaterial induced by negative Poisson's ratio property. Mater. Des. *192*, 108751. https://doi.org/10.1016/j.matdes.2020.108751.

21. Tan, X., Cao, B., Liu, W., Ji, C., Wang, B., and Li, S. (2024). Odd mechanical metamaterials with simultaneously expanding or contracting under both compression and tension. Thin-Walled Struct. *203*, 112225. https://doi.org/10.1016/j.tws.2024.112225.

22. Chenal, T., Case, J., Paik, J., and Kramer, R. (2014). Variable Stiffness Fabrics with Embedded Shape Memory Materials for Wearable Applications. In 2014 IEEE/RSJ International Conference on Intelligent Robots and Systems., pp. 2827–2831. https://doi.org/10.1109/IROS.2014.6942950.

23. Baines, R., Patiballa, S.K., Booth, J., Ramirez, L., Sipple, T., Garcia, A., Fish, F., and Kramer-Bottiglio, R. (2022). Multi-environment robotic transitions through adaptive morphogenesis. Nature *610*, 283–289. https://doi.org/10.1038/s41586-022-05188-w.

24. Tonazzini, A., Mintchev, S., Schubert, B., Mazzolai, B., Shintake, J., and Floreano, D. (2016). Variable Stiffness Fiber with Self-Healing Capability. Adv. Mater. *28*, 10142–10148. https://doi.org/10.1002/adma.201602580.

25. Kim, Y.J., Cheng, S., Kim, S., and Iagnemma, K. (2014). A stiffness-adjustable hyperredundant manipulator using a variable neutral-line mechanism for minimally invasive surgery. IEEE Trans. Robot. *30*, 382–395. https://doi.org/10.1109/TRO.2013.2287975.

26. Xie, M., Hisano, K., Zhu, M., Toyoshi, T., Pan, M., Okada, S., Tsutsumi, O., Kawamura, S., and Bowen, C. (2019). Flexible Multifunctional Sensors for Wearable and Robotic Applications. Adv. Mater. Technol. *4*, 1–29. https://doi.org/10.1002/admt.201800626.

27. Gillespie M., Best C., Killpack M. Simultaneous Position and Stiffness Control for an Inflatable Soft Robot. 2016 IEEE International Conference on Robotics and Automation (ICRA), Stockholm, Sweden. (2016); 1095-1101. https://doi.org/10.1109/ICRA.2016.7487240.

28. Tonietti G., Bicchi A. Adaptive simultaneous position and stiffness control for a soft robot arm. IEEE/RSJ International Conference on Intelligent Robots and Systems, Lausanne, Switzerland. (2002); 1992-1997 vol.2, https://doi.org/10.1109/IRDS.2002.1044048.

29. Kim, Y.J., Cheng, S., Kim, S., and Iagnemma, K. (2013). A novel layer jamming mechanism with tunable stiffness capability for minimally invasive surgery. IEEE Trans. Robot. *29*, 1031–1042. https://doi.org/10.1109/TRO.2013.2256313.

30. Ou J., Yao L., Tauber D., Steimle J., Niiyama R., Ishii H. jamSheets: Thin interfaces with tunable stiffness enabled by layer jamming. 8th International Conference on Tangible, Embedded and Embodied Interaction (TEI '14). Association for Computing Machinery. 65–72. https://doi.org/10.1145/2540930.2540971.

31. Li, Y., Chen, Y., Yang, Y., and Wei, Y. (2017). Passive Particle Jamming and Its Stiffening of Soft Robotic Grippers. IEEE Trans. Robot. *33*, 446–455. https://doi.org/10.1109/TRO.2016.2636899.

32. Brown, E., Rodenberg, N., Amend, J., Mozeika, A., Steltz, E., Zakin, M.R., Lipson, H., and Jaeger, H.M. (2010). Universal robotic gripper based on the jamming of granular material. Proc. Natl. Acad. Sci. USA *107*, 18809–18814. https://doi.org/10.1073/pnas.1003250107.

33. Buckner, T.L., Yuen, M.C., and Kramer-Bottiglio, R. (2020). Shape Memory Silicone Using Phase-Changing Inclusions. 2020 3rd IEEE International Conference on Soft Robotics (RoboSoft), 259–265. https://doi.org/10.1109/RoboSoft48309.2020.9116008.

34. Bilodeau, R.A., Yuen, M.C., and Kramer-Bottiglio, R. (2019). Addressable, Stretchable Heating Silicone Sheets. Adv. Mater. Technol. *4*, 1–11. https://doi.org/10.1002/admt.201900276.

35. Bilodeau, R.A., Mohammadi Nasab, A., Shah, D.S., and Kramer-Bottiglio, R. (2020). Uniform Conductivity in Stretchable Silicones via Multiphase Inclusions. Soft Matter *16*, 5827–5839. https://doi.org/10.1039/d0sm00383b.

36. Sudheer, M., K, R.,P., and Somayaji, S. (2015). Analytical and Numerical Validation of Epoxy/Glass Structural Composites for Elastic Models. Am. J. Mater. Sci. *5*, 162–168. https://doi.org/10.5923/c.materials.201502.32.

37. Halpin, J.C., and Kardos, J.L. (1976). The Halpin-Tsai equations: A review. Polym. Eng. Sci. *16*, 344–352. https://doi.org/10.1002/pen.760160512.

38. Chawla, K.K. (2012). Micromechanics of composites. In Composite materials (Springer), pp. 337–386. https://doi.org/10.1007/978-0-387-74365-3.

39. Peng, X.L., Soyarslan, C., and Bargmann, S. (2020). Phase contrast mediated switch of auxetic mechanism in composites of infilled re-entrant honeycomb microstructures. Extreme Mech. Lett. *35*, 100641. https://doi.org/10.1016/j.eml.2020.100641.

40. Laufer, Z., Diamant, Y., Gill, M., and Fortuna, G. (1978). A Simple Dilatometric Method for Determining Poisson's Ratio of Nearly Incompressible Elastomers. International Journal of Polymeric Materials and Polymeric Biomaterials *6*, 159–174. https://doi.org/10.1080/00914037808077906.

41. Buckner, T.L., Yuen, M.C., Kim, S.Y., and Kramer-Bottiglio, R. (2019). Enhanced Variable Stiffness and Variable Stretchability Enabled by Phase-Changing Particulate Additives. Adv. Funct. Mater. *29*, 1903368. https://doi.org/10.1002/adfm.201903368.

42. Shintake, J., Piskarev, Y., Jeong, S.H., and Floreano, D. (2018). Ultrastretchable strain sensors using carbon black-filled elastomer composites and comparison of capacitive versus resistive sensors. Adv. Mater. Technol. *3*, 1700284. https://doi.org/10.1002/admt.201700284.

43. Porte, E., and Kramer-Bottiglio, R. (2021). Nonlinear Poisson's Ratio for Modeling Hyperelastic Capacitive Sensors. Adv. Mater. Technol. *6*, 2001247. https://doi.org/10.1002/admt.202001247.

44. Tairych, A., and Anderson, I.A. (2019). Capacitive stretch sensing for robotic skins. Soft Robot. *6*, 389–398. https://doi.org/10.1089/soro.2018.0055.

45. Buckner, T.L., Yuen, M.C., Kim, S.Y., and Kramer-Bottiglio, R. (2019). Enhanced Variable Stiffness and Variable Stretchability Enabled by Phase-Changing Particulate Additives. Adv. Funct. Mater. *29*, 1–10. https://doi.org/10.1002/adfm.201903368.

46. Buckner, T.L., Farrell, Z.J., Nasab, A.M., and Kramer-Bottiglio, R. (2023). Effects of particle size and oxide shell on variable stiffness performance of phase-changing materials. J. Compos. Mater. *57*, 619–631. https://doi.org/10.1177/00219983221129252.

47. Porte, E., Sipple, T., Sanchez Botero, L., Shah, D., and Kramer-Bottiglio, R. (2021). Capacitive sensor measurement rate improves by pre-stretching. 2021 IEEE 4th International Conference on Soft Robotics (RoboSoft)., 412–418. https://doi.org/10.1109/RoboSoft51838.2021.9479328.

48. White, E.L., Yuen, M.C., Case, J.C., and Kramer, R.K. (2017). Low-cost, facile, and scalable manufacturing of capacitive sensors for soft systems. Adv. Mater. Technol. *2*, 1700072. https://doi.org/10.1002/admt.201700072.